HHS Public Access

Author manuscript

J Mol Cell Cardiol. Author manuscript; available in PMC 2015 November 01.

Published in final edited form as:

J Mol Cell Cardiol. 2014 November ; 76: 84–93. doi:10.1016/j.yjmcc.2014.07.020.

Caveolin-1 deletion exacerbates cardiac interstitial fibrosis by promoting M2 macrophage activation in mice after myocardial infarction

Pooja Shivshankar[a], **Ganesh V. Halade**[a,1], **Cheresa Calhoun**[a], **Gladys P. Escobar**[a], **Ali J. Mehr**[a], **Fabio Jimenez**[a], **Cindy Martinez**[a], **Harshita Bhatnagar**[a], **Corey H. Mjaatvedt**[b], **Merry L. Lindsey**[a,2], and **Claude Jourdan Le Saux**[a,*]

[a]Division of Cardiology, Department of Medicine, University of Texas Health Science Center at San Antonio, San Antonio, TX 78229, USA

[b]Department of Regenerative Medicine & Cell Biology, Medical University of South Carolina, Charleston, SC 29425, USA

Abstract

Adverse remodeling following myocardial infarction (MI) leading to heart failure is driven by an imbalanced resolution of inflammation. The macrophage cell is an important control of post-MI inflammation, as macrophage subtypes secrete mediators to either promote inflammation and extend injury (M1 phenotype) or suppress inflammation and promote scar formation (M2 phenotype). We have previously shown that the absence of caveolin-1 (Cav1), a membrane scaffolding protein, is associated with adverse cardiac remodeling in mice, but the mechanisms responsible remain to be elucidated. We explore here the role of Cav1 in the activation of macrophages using wild type C57BL6/J (WT) and *Cav1*$^{tm1Mls/J}$ (*Cav1*$^{-/-}$) mice. By echocardiography, cardiac function was comparable between WT and *Cav1*$^{-/-}$ mice at 3 days post-MI. In the absence of Cav1, there were a surprisingly higher percentage of M2 macrophages (arginase-1 positive) detected in the infarcted zone. Conversely, restoring Cav1 function after MI in WT mice by adding back the Cav1 scaffolding domain reduced the M2 activation profile. Further, adoptive transfer of Cav1 null macrophages into WT mice on d3 post-MI exacerbated adverse cardiac remodeling at d14 post-MI. In vitro studies revealed that Cav1 null macrophages had a more pronounced M2 profile activation in response to IL-4 stimulation. In conclusion, Cav1 deletion promotes an array of maladaptive repair processes after MI, including increased TGF-β signaling, increased M2 macrophage infiltration and dysregulation of the M1/M2 balance. Our

*Corresponding author at: Department of Medicine, Division of Cardiology, University of Texas Health Science Center at San Antonio, 7703 Floyd Curl Drive, San Antonio, TX 78229, USA. Tel.: +1 210 567 4614; fax: +1 210 567 6960. lesaux@uthscsa.edu (C.J. Le Saux).

[1]GVH is now at: Division of Cardiovascular Disease, Department of Medicine, University of Alabama at Birmingham, AL 35233, USA.

[2]MLL is now at: Mississippi Center for Heart Research, Department of Physiology and Biophysics, University of Mississippi Medical Center, Jackson, MS 39216, USA.

Conflict of interest

None.

Appendix A. Supplementary data

Supplementary data to this article can be found online at http://dx.doi.org/10.1016/j.yjmcc.2014.07.020.

data also suggest that cardiac remodeling can be improved by therapeutic intervention regulating Cav1 function during the inflammatory response phase.

Keywords

Myocardial infarction; Caveolin-1; Transforming growth factor β1 (TGF-β1); Inflammation; Macrophage polarization; Interstitial fibrosis

1. Introduction

Myocardial infarction (MI) occurs as a result of ischemic damage to the left ventricle (LV) [1,2]. Within hours following ischemia, an acute inflammatory response is initiated, with neutrophils infiltrating the necrotic area first, followed by infiltration of macrophages days later [3,4]. Macrophages secrete mediators to promote or suppress inflammation and to regulate the LV remodeling wound healing response. There are two major subsets of macrophages: classically activated M1 that secretes large amounts of pro-inflammatory mediators and alternatively activated M2 macrophages that dampen the inflammatory response and promote tissue remodeling and repair [5,6]. Not only is the contribution of these different subpopulations of macrophages to the proper healing process not well understood, but also is the regulation of macrophage differentiation largely unknown.

Among the mediators that are implicated in macrophage differentiation, Transforming growth factor (TGF)-β1 has been proposed to shift macrophage polarity to an alternatively activated phenotype (M2) [7]. While TGF-β1 activity has beneficial aspects in stimulating scar formation to provide structural strength to the myocardium, TGF-β1 can also further damage the surrounding normal tissue by stimulating fibrosis that can increase LV stiffness and further reduce LV function [8]. Thus an optimal level of TGF-β1 signaling must be curtailed to balance the inflammatory response while preserving normal LV function.

Caveolin-1 (Cav1) is a major membrane-bound protein that forms omega-shaped structures called caveolae that are present in the majority of differentiated cells [9]. We have recently shown that Cav1 regulates TGF-β1 signaling and cardiac remodeling following myocardial injury in mice [10]. Regulation by Cav1 occurs by internalizing the TGF-β1 receptor (TGFβR) within the caveolae and by direct interaction of cav1 with the inhibitory Smad2/3 complex. Sequestration of TGFβRs by Cav1 is facilitated by the inhibitory Smad, Smad7 [11,12]. While the role of Cav1 in the regulation of inflammation is still under investigation, Cav1 has been shown to play a critical role in the differentiation of monocytes into macrophages [13].

Accordingly, we hypothesized that Cav1 is involved in the regulation of the inflammatory response to MI by regulating macrophage differentiation. We tested this hypothesis using a mouse model of permanent coronary artery ligation. We evaluated inflammatory responses by histology, cellular invasion, alteration in macrophage phenotypes, and corresponding cytokine levels released post-MI. Additionally, in vitro studies were performed to determine howCav1 influences macrophage polarization to regulate pro-fibrotic mediators that stimulate fibroblast activation and collagen deposition.

2. Materials and methods

2.1. Mouse strains and procedure

Breeding pairs of wild-type (WT) C57BL/6J and Cav$^{tm1Mls/J}$ (*Cav1*$^{-/-}$) mice were purchased from Jackson Laboratory (Bar Harbor, Maine) and used to establish breeding colonies. Animal experiments were conducted in compliance with a protocol approved by the Institutional Animal Care and Use Committee of the University of Texas Health Science Center, San Antonio.

In experimental groups, MI was induced by surgical ligation of the left anterior descending coronary artery as previously described [14]. Control groups were consisted of 8 week-old male WT and *Cav1*$^{-/-}$ mice with no MI.

A subgroup of WT mice was treated for 3 days after MI with the caveolin-1 scaffolding domain (CSD) or scrambled peptide (Scr), at a final concentration of 0.5 mM in 10% DMSO delivered by Alzet osmotic minipumps (0.5 μl per hour for one week (Model #1007D, Durect Corporation, Cupertino, CA) as described by Miyasato et al. [10]. A second subgroup of WT and *Cav1*$^{-/-}$ mice (n = 5) were treated 24 h post-MI with intraperitoneal (ip) administration of anti-TGF-β antibody or the isotype control (R&D Systems, Minneapolis, MN) at a dose of 10 mg/kg body weight.

Another group was subjected to an adoptive transfer of bone marrow derived macrophages extracted from either WT or *Cav1*$^{-/-}$ mice. Briefly, as described elsewhere, two washes of 0.5 ml of 10% FBS-RPMI supplemented with antibiotics were used to flush bone marrow cells from the femur and tibia bones of the WT and *Cav1*$^{-/-}$ mice, and subjected to centrifugation (10 min; 500 ×g) to collect the cell fraction. The monocytes/macrophages were isolated using the mouse CD115 microbeads (Miltenyi Biotech, Auburn, CA) following manufacturer's directions. The purified cells were injected intravenously (2×10^6 cells/mouse) through the jugular vein of the coronary ligated WT or *Cav1*$^{-/-}$ mice. Mice were sacrificed and heart tissues were collected 14 days after MI to assess collagen deposition and the presence of CD45$^+$ (leukocyte marker) and Hsp47$^+$ (collagen producing cell marker) cells in the myocardium.

After 3 days of permanent ligation, all WT and *Cav1*$^{-/-}$ mice underwent echocardiographic assessment [14]. Echocardiograms were acquired under spontaneous respiration with 0.5–1% isoflurane in an oxygen mix. Electrocardiogram and the heart rates were monitored throughout the imaging procedure using a surface electrocardiogram (Vevo 770® High-Resolution In Vivo Imaging System Visual Sonics). Images were taken with heart rates more than 400 beats/min to maintain physiological relevance. Measurements were taken from the two-dimensional parasternal long and short-axis recordings of the LV. For each parameter, 3 consecutive images were measured and averaged. One and three days after myocardial injury by coronary ligation, mice were sacrificed for tissue collection.

2.2. Cardiac tissue collection

Mice were anesthetized using isoflurane, and the LV was flushed with cardioplegic solution [15]. The hearts were excised and the LV and right ventricle (RV) were separated and

weighed separately. The LV was sectioned into three regions—apex, mid-cavity, and base. These sections were stained with 1% 2,3,5-triphenyltetrazolium chloride (Sigma-Aldrich, St Louis, MO) to quantify infarct area. The infarcted and remote regions from the apex and base were snap-frozen and stored separately at −80 °C for further biochemical analysis. The midcavity was fixed in 10% zinc formalin for histological examination. Left ventricle (LV) tissues were collected 1 or 3 days following MI. Tissues from animals that had died spontaneously before sacrifice were not included for further studies.

2.3. Histology, immunohistochemistry, and evaluation of cell infiltration

Post-fixation, the LV mid-cavity was embedded in paraffin. Sections were cut 3 μm thick and stained with hematoxylin and eosin. Paraffin-embedded tissue sections were stained with Ly6B.2 (AbD Serotec, Raleigh, NC), anti-Mac-2 (Cedarlane, Burlington, NC), and arginase-1 (Santa Cruz Biotechnoly Inc., Santa Cruz, CA) for neutrophils, macrophages, and alternatively activated macrophages per manufacturer's instructions. At least 4 random fields per section were acquired from at least 2 sections per mouse. Cells were counted by blinded analysis at a total magnification of 200×.

2.4. Gene and protein expression

Total LV RNA was extracted from infarcted LV samples using the RNeasy™ kit (Qiagen Inc., Valencia, VA). Equal quantities of RNA (200 ng) were converted into first-strand cDNA using random hexamers (SuperScript III First-Strand Synthesis System for RT-PCR™, Invitrogen Life Technologies, Grand Island, NY). The mRNA abundance for 84 different genes associated with inflammation was checked using RT^2 Profiler™ PCR Array (SABiosciences, Valencia, CA). Specific gene levels that showed two or more fold changes were secondarily analyzed by RT-PCR (qPCR) using commercially available TaqMan probes (Applied Biosystems, Carlsbard, CA). Results were analyzed by the ΔΔCt method with 18 s rRNA as the internal control.

For immunoblot analyses, modified RIPA buffer was used to extract total protein from frozen LV tissues. Protein samples of 30 μg from individual hearts were electrophoresed on a 4–15% SDS-PAGE gel, as previously described [16,17]. Briefly, separated proteins were transferred to nitrocellulose membranes, blocked for non-specific protein binding using 5% BSA in 50 mM Tris, pH7.2/150 mM NaCl/0.5% Tween 20 (TBST), and probed for selected proteins with a specific primary antibody followed by a secondary peroxidase labeled antibody for detection. Primary antibodies used were against anti-Smad2 (Cell signaling, Billerica, MA), anti-phospho-Smad2 (Cell signaling), and Smad-7 (Cell Signaling). The appropriate peroxidase-linked secondary antibodies were detected using ECL Plus (Pierce). Multiple exposures of X-ray film were made with the ECL treated membrane to assure that the developed band densities were within the linear range. Measurements to determine the relative densities were normalized to standard protein (GAPDH or β-actin) using NIH image J software [18].

2.5. Picosirius red staining for collagen deposition and fibrocyte detection

Paraffin-embedded cardiac tissue sections were stained with picrosirius red (PSR) for collagen. Briefly, cardiac tissue sections were de-waxed and rehydrated to distilled water.

Samples were then incubated in 500 μl of phosphomolybdic Acid 0.2% (cat. No 26356-01 Electron Microscopy Science, Hatfield, PA 19440) for 5 min at room temperature. Following incubation, the tissue sections were directly placed in sirius red 0.2% in saturated picric acid (cat. No 26357-02; Electron Microscopy Science) for 90 min at room temperature. Tissue sections were finally washed in 0.01 N hydrochloric acid for 2 min and fixed in 70% alcohol for 45 s. The extent of PSR staining was visualized and images were acquired using the Olympus CKS41 inverted light microscopy equipped with CellSens Dimension Software (Olympus America Inc., Center Valley, PA).

For immunohistochemical detection of fibrocytes, sections were pretreated to unmask cryptic antigens using a high-temperature citric acid solution according to manufacturer's directions (H-3300, Vector Laboratories, Burlingame, CA). Sections were blocked 1 h at room temperature with blocking buffer (PBS, Sigma) containing 3% bovine serum albumin (catalog no. B4287, Sigma) then incubated 12 h at 4 °C with primary antibody diluted in blocking buffer (1/500 anti-CD45, Santa Cruz Biotechnology and Hsp47, MBL international). After primary antibody incubations, specimens were washed (3 times 10 min each) in PBS and incubated at room temperature with fluorochrome-conjugated secondary antibody (Alexa 488 or 594; Jackson Immunoresearch, West Grove, PA) diluted 1/500 in blocking buffer. All samples were washed extensively in PBS and slides were coverslipped using DABCO mounting media (Sigma). Controls included the use of the secondary antibody only. Immunostained sections were analyzed using a Leica TCS SP5 AOBS Confocal Microscope System (Leica Microsystems, Inc., Exton, PA).

2.6. Peritoneal macrophage purification and stimulation

Two-month old male WT and *Cav1*$^{-/-}$ mice were injected with 5–10 ml of RPMI with 2% FBS into the peritoneal cavity and media was removed. All cells were collected, spun down, counted, and plated to achieve an equivalent concentration per well (1×10^6 cells per well). For the isolation of the cells from the peritoneal cavity, cells were differentiated by media selection (composed of 1% HEPES, 1% penicillin/ streptomycin, 10% L929 cell conditional medium [F-12/DMEM/10% fetal bovine serum], 10% fetal bovine serum, and 2 mM L-glutamine). Once confluent, macrophages were stimulated for 24 h with IL-4 (10 ng/ml). The supernatant was stored at −80 °C until use for the treatment of fibroblasts in subsequent assays.

Arginase activity was quantified by measuring the conversion of L-arginine into urea as previously reported [19]. In brief, 10 mM $MnCl_2$ in 50 mM Tris–HCl was added to the lysed sample and the mixture was then incubated at 56 °C to activate the arginase enzyme. L-Arginine was then added and samples were incubated at 37 °C for 2 h and terminated by the addition of an acid solution. The colorimetric indicator, 6% α-isonitrosopropiophenone in 100% ethanol, was then added to each tube, heated to 95 °C, and the OD of each sample was read at the wave-length of 540 nm. Arginase activity in the samples was determined based on the standard curve of known urea concentration.

2.7. Statistical analysis

Comparison of the survival curves was analyzed using log-rank (Mantel Cox) test. Other results were expressed as mean ± standard error of mean. A two-way ANOVA followed by Bonferroni post-test was used to perform a comparison between multiple groups to assess the effect of the genotype and the injury. A p-value < 0.05 was considered significant. Data entry, management, and statistical analysis were performed using Prism software (GraphPad Software, La Jolla, CA). The *t*-test was used for all 2-group comparisons.

3. Results

3.1. Absence of caveolin-1 results in reduced survival and increased immune cell infiltrate after MI

We first determined the effect of MI on the WT and *Cav1*$^{-/-}$ mice in terms of survival analysis and pathology assessment. As previously shown, Cav1 expression transiently decreased in WT animals [10]. To rescue normal function, Cav1 scaffolding domain was delivered to WT mice after MI. Interestingly, all WT mice survived to 3 days post-MI, whereas *Cav1*$^{-/-}$ mice had a poor survival rate and exhibited significant steady declines in survival of 95%, 82%, and 47% on days 1, 2, and 3, respectively (p = 0.0086 when WT 3 days is compared to *Cav1*$^{-/-}$ 3 days), despite infarct areas not being significantly different between WT (51 ± 1% infarct area) and the surviving *Cav1*$^{-/-}$(49 ± 4% infarct) mice (Table 1). The fact that infarct areas were similar demonstrated that the cardiac injury stimulus given was equal for the two groups. While normal tissue architecture was observed in WT control mice, a pronounced increase in inflammatory cells was observed by day 3 (Fig. 1B). Three days after cardiac injury, the gross morphological characteristics did not differ among the surviving WT, CSD- or Scr-treated WT mice, and *Cav1*$^{-/-}$ groups (Fig. 1C). Within the first three days after injury, most of the *Cav1*$^{-/-}$ mice (87.5%) died from myocardial rupture and 12.5% were found with edematous lungs.

3.2. Caveolin-1 deficiency does not alter LV function, dimension, and volume compared to WT

In the first three days of myocardial infarction, Caveolin-1 deficient (*Cav1*$^{-/-}$) does not alter function of the left ventricle (LV). Fractional shortening (FS%), ejection fraction (EF%), and LV posterior wall thickness in systole (LV PWTs) and LV posterior wall thickness in diastole (LV PWTd) are not statistically different between WT and *Cav1*$^{-/-}$ mice. As expected, LV function evaluated by FS% was reduced after cardiac injury in WT and *Cav1*$^{-/-}$ mice, suggesting that Cav1 deficiency did not promote a worsening of the LV function within the first three days after LAD ligation (Table 1). Parameters measured to assess cardiac dimension LV PWTd, LV PWTs and volume end-diastolic volume (EDV), end-systolic volume (ESV), and EF% indicated that the deficiency in *Cav1* did not affect the cardiac response to injury (Table 1).

These data suggested that the increase mortality in the *Cav1*$^{-/-}$ mice did not occur as the result of alteration of the early cardiac function, dimension, and volume associated with cardiac injury but rather to the increased inflammatory responses.

3.3. Caveolin-1 deficiency promotes altered inflammatory responses following MI

Neutrophils and macrophages have been shown to be the major inflammatory cell types involved in post-injury cardiac events. Thus, we assessed changes in these infiltrating cells in the infarcted zone. Normal tissue architecture with the absence of inflammatory cells was noted for the WT and *Cav1*$^{-/-}$ control mice (Fig. 1B). Both WT and *Cav1*$^{-/-}$ mice presented a significant increase in neutrophil infiltration one day after MI. Both strains showed comparable clearance of neutrophils 3 days post-MI. The treatment with CSD did not affect neutrophil infiltration and clearance in both mouse strains (Supplemental Fig. 1).

Macrophages were absent at baseline, but a significant increase in macrophage density was observed within the infarcted myocardium for all the groups by day 3 post-MI, further enhanced in *Cav1*$^{-/-}$ animals (Figs. 2A,D). Assessment of arginase-1-positivemacrophage recruitment similarly revealed the absence of infiltration on days 0 in WT mice, with a significant increase on day 3 post-MI that was further enhanced in *Cav1*$^{-/-}$ mice (Figs. 2B, D). Moreover, the percentage of arginase-1 positive macrophages was reduced by 1.5-fold in the CSD-treated WT mice ($p < 0.05$) (Fig. 2A). Supportive of these data, the level of expression of arginase-1 mRNA was upregulated following MI in WT mice and further enhanced in *Cav1*$^{-/-}$ mice (Fig. 2C).

Due to the importance of the inflammatory response in the regulation of post-MI LV remodeling, we explored the level of expression of cytokines that have been shown to be involved in the progression of MI. As expected from the work from Wang et al. [20], Cav1 deletion affects the expression profile of classic macrophage markers. Three days after cardiac injury, *IL-1*β and *mcp-1* mRNA expression showed an increase in the infarcted WT heart tissue that was further up-regulated in *Cav1*$^{-/-}$ mice (Fig. 3A). Because of the importance of IL-4 in promoting M2 macrophage phenotype, the mRNA level of this cytokine was assessed. The level of IL-4 expression was increased in WT in the LV infarct 3 days after injury and significantly enhanced in injured *Cav1*$^{-/-}$ mice (Fig. 3B). Of the M2 markers measured, *arginase-1* and *TGF*-β mRNA were increased after MI and further enhanced in *Cav1*$^{-/-}$ mice, while *Ym1* mRNA level increased after MI but with no statistical difference between the 2 strains (Fig. 3B).

3.4. Adoptive transfer of Cav1 deficient macrophages promotes interstitial fibrosis after MI

To further explore whether a Cav1 deletion, specifically in macrophages, results in enhanced M2 phenotype and induction of the pro-fibrotic responses from fibroblasts that mediate the adverse cardiac remodeling as indicated by interstitial collagen associated with the presence of fibrocytes, *Cav1*$^{-/-}$ macrophages were adoptively transferred into recipient WT mice. Conversely, WT macrophages were adoptively transferred into *Cav1*$^{-/-}$ mice 3 days after MI. This is the post-MI time period in our model when macrophages begin invading and differentiating within the myocardium. Interestingly, WT mice receiving *Cav1*$^{-/-}$ macrophages showed decreased survival (50% of the mice died compared to 33% when the WT mice receive WT macrophages). Moreover *Cav1*$^{-/-}$ mice receiving WT macrophages showed increased survival (67% compared to 50% when the *Cav1*$^{-/-}$ mice received *Cav1*$^{-/-}$ macrophages). All of the non-surviving mice died from cardiac rupture within the first week after the adoptive transfer. Histological analysis showed that the *Cav1*$^{-/-}$ macrophage

adoptive transfer led to the worsening of fibrosis deposition that resembled the interstitial fibrosis found in Cav1$^{-/-}$ mice 14 days after MI, shown both as an increase in percentage of collagen in the infarct region and presence of collagen in the myocardial interstitium. In contrast, WT macrophages transfer ameliorated the development of interstitial fibrosis detected in *Cav1*$^{-/-}$ mice as indicated by collagen deposition and the absence of fibrocytes (Fig. 4). These data further confirmed the pathological role of Cav1 deletion in macrophages during the development and progression of adverse remodeling observed in *Cav1*$^{-/-}$ mice after MI.

3.5. In vitro IL-4 stimulation skewed Cav1$^{-/-}$ macrophages toward M2 polarization

To further investigate the impact of Cav1 deletion on macrophage phenotypic activation, peritoneal macrophages were stimulated with IL-4 to promote M2 macrophage activation. We characterized the activation of M2 macrophage phenotype using a functional assay (arginase enzymatic assay) and the level of mRNA expression of M2 markers. Compared with WT, IL-4 stimulated *Cav1*$^{-/-}$ macrophages showed an enhanced arginase enzymatic assay activation (Fig. 5A, $p < 0.05$). This characteristic M2 response was mirrored by a significant increase in the mRNA expression of *arg1*, *fizz1*, and *Ym1* (Fig. 5B, all $p < 0.05$).

3.6. Caveolin-1-dependent regulation of TGF-β signaling promotes the M2 macrophage phenotype

To determine the extent to which Cav1 regulates the TGF-β-dependent anti-inflammatory function after MI, we analyzed the level of expression of 84 different genes associated with inflammation by real-time PCR. Thirty five percent of all the genes analyzed were TGF- β-dependent. Of the TGF-β-dependent genes, 70% was also Cav1- dependent, thus being regulated by *both* TGF-β and Cav1. Another group of genes (14%) was uniquely Cav1 expression-dependent. We confirmed that *IL-4* and *IL-17*β mRNA levels were upregulated in the absence of Cav1 and downregulated after anti-TGF-β treatment indicating that the absence of Cav1 could also play a critical regulatory role in the induction of M2 profiling by regulating the level of IL-4 (Fig. 6).

TGF-β signaling activation was assessed by the level of phosphrylation of Smad2, one of the main transduction proteins in the TGF-β canonical signaling pathway. As expected, in WT animals, increased pSmad2 levels were measured 3 days post-injury. In contrast, these levels were significantly decreased in CSD-treated groups (Supplemental Fig. 2).

To elucidate if the reduced percentage of M2 macrophages in the total macrophage population measured after CSD treatment was the result of reduced TGF-β signaling, WT mice were treated after MI with anti-TGF-β antibody. Neutralization of TGF-β function in the WT mice resulted in a two-fold decrease in the arginase-1-positive macrophage within the injured LV (Figs. 7A, B) and reduction of the ratio of pSmad2/total Smad2 as a reflection of TGF-β signaling dampening (Fig. 7 over representation of M2 macrophages and their potential for promoting). Overall, the downregulation of TGF-β signaling by CSD or anti-TGF-β therapy resulted in a decreasedM2 macrophage proportion of the total macrophage population.

4. Discussion

The goal of this study was to evaluate the role of Cav1 in post-MI remodeling. The most significant findings were: 1) After MI, the absence of Cav1 promotes an increase in macrophage infiltration and cardiac fibrosis, specifically augmenting the proportion of the M2 macrophage population 2); M2 activation profile is enhanced in vitro in the absence of Cav1 and; 3) Caveolin-1 rescue or TGFβ neutralization reverses this phenotype. Combined, our results demonstrate for the first time that Cav1 participates in the inflammatory responses following MI in mice. Furthermore, our studies support the role of Cav1 in regulating an array of adaptive repair processes, with effects on macrophage activation being a predominant effect. More importantly, the balance between M1/M2 macrophages is altered by Cav1 deficiency, with an excess ofM2 macrophages at an earlier than expected time frame leading to impaired repair mechanisms following MI.

At baseline, no significant differences were observed between WT and the surviving *Cav1*$^{-/-}$, in terms of LV structure and function. Consistent with the previous reports, our data indicated reduced survival and impaired cardiac function of *Cav1*$^{-/-}$ mice within 24 h after permanent coronary ligation despite equal infarct areas, mainly due to LV rupture [21]. It is important to note that this high rate of mortality could potentially be a caveat, as we therefore studied the survivors. LV rupture can occur within the first 48 h after MI without being associated with a significant wall thinning or regional remodeling, as we observed, in contrast to the rupture occurring within 3 to 10 days after MI [22–24]. The early rupture has been shown to happen as a consequence of deficient post-MI inflammation due to weakening of tensile strength [25]. Another critical factor is the size of the infarction. This factor was not an issue in the current study, because both strains had comparable infarct sizes; this indicates that the dramatic differences in inflammatory profiles were likely the reason for the differences in survival rates. Since the role of Cav1 in acute inflammatory responses following cardiac injury had not been previously addressed, we measured an increased level of MCP-1 mRNA expression in *Cav1*$^{-/-}$ mice 3 days after injury. MCP-1 plays a critical role in the immediate responses following MI [26]. Neutralizing MCP-1 has been shown to significantly reduce infarct size and macrophage infiltration [27]. In our model, this increase of MCP-1 mRNA expression could contribute to the decreased survival in *Cav1*$^{-/-}$ mice compared to WT mice.

Cav1 deletion leads to a relative increase inM2 macrophage population within 3 days after cardiac injury, which is earlier than the normal course. During this acute phase of inflammation, the M1 population of macrophages is usually predominant. In contrast, the M2 macrophage population is found later during scar formation as measured by increased *arg-1* and *TGF*-β mRNA. Given the fact that there is a preferential M2 macrophage polarization, it is interesting that 3 days after MI, the level of *IL-4* mRNA was significantly increased compared to the baseline in *Cav1*$^{-/-}$mice. Our in vitro data clearly showed that upon IL-4 stimulation, peritoneal macrophages carrying the Cav1 deletion responded with a significantly greater level of conversion to M2 polarization. The over representation of M2 macrophages in *Cav1*$^{-/-}$ most likely contributes to the adverse remodeling measured 14 days after injury that we have previously demonstrated [10]. Indeed, adoptive transfer of M2 macrophages not expressing Cav1 leads to the development of extensive interstitial fibrosis

in WT mice beyond the expected healthy fibrous scar formation necessary to fill the wound and maintain normal wall integrity while the cardiomyocytes are partially replaced [28]. In agreement with these observations, the parallel experiments in which *Cav1*$^{-/-}$ injured mice received WT macrophages by adoptive transfer showed that they developed only limited interstitial fibrosis during the same period of time after MI.

A critical role in the pathogenesis of cardiac remodeling through the effects on inflammatory and reparative responses has been attributed to TGF-β. It may be the master switch mediating the transition from inflammation to scar formation following myocardial infarction [8]. Early TGF-β antagonism through transfection with the extracellular domain of its receptor or early treatment with a neutralizing anti-TGF-β antibody within 24 h following coronary occlusion increased mortality due to enhanced inflammation [29,30].

Despite the evidence of an abundance of macrophages in the infarcted heart and their potential for the regulation of the inflammatory response, our knowledge of the role of these macrophages remains limited [31–33]. Two distinctive macrophage subsets have been recognized; the classically activated M1 macrophages that secrete proinflammatory mediators, and alternatively activated M2 macrophages that show increased phagocytic and anti-inflammatory activities [34, 35]. Generally, arg-1-positive M2 macrophages are considered profibrotic, and the arg-1 negative population is believed to trigger potential anti-inflammatory response [36]. Arg-1 has recently reported to be indirectly related to fibrosis development by promoting the release of Th2-dependent cytokines (IL-10 and TGF-β1) and also shown to promote Th1 response [37]. In our study, an increase of arg-1-positivemacrophages was observed in WT and *Cav1*$^{-/-}$ mice at day 3 post-MI. This increase was much higher in the *Cav1*$^{-/-}$ group of mice. An increased number of arg-1-positive macrophages among *Cav1*$^{-/-}$ mice and anti-TGF-β antibody-treated mice correlated with the highest mortality rate among these two groups. The disproportionate increase of arg-1-positive macrophage numbers might predispose the injured hearts to maladaptive remodeling and cardiac fibrosis, leading to increased mortality post-MI in these groups.

The inflammation specific gene expression array data revealed that some of the genes regulated by Cav1were not TGF-β1-dependent, suggesting that infarction-induced acute inflammation and pathogenesis may involve a mixed response. IL-10, IL-4, and IL-1R2 are among the most important anti-inflammatory cytokines that are released post-MI. IL-4 is reported to antagonize the activity of IL-1β by inducing the expression and release of IL-1R2, which binds to IL-1α and IL-1β and acts as a decoy receptor and inhibits the activity of its ligands. Exposure to IL-4 also programs macrophages to M2 macrophages [6]. IL-10 inhibits proinflammatory cytokines such as IL-1, IL-6, and TNF-α produced by macrophages [32]. We compared the mRNA expression of IL-10, IL-4, and IL-R2 between WT and *Cav1*$^{-/-}$ mice. These cytokines are the key components in M2 macrophage induction and maturation pathways. When these anti-inflammatory cytokine gene expression profiles were compared with the chemotaxis of M2 macrophages in post-MI cardiac tissues, we noticed, as expected, a concordant increase of their gene expression with the increase in theM2macrophage population among *Cav1*$^{-/-}$ mice and anti-TGF-β antibody-treated WT mice. As M2 macrophages have been characterized as being profibrotic, it is important to

note that we previously demonstrated that, in the absence of Cav1, cardiac remodeling was more pronounced [10].

A better understanding of the inflammatory mechanisms operating during myocardial infarction healing is very important as it could lead to more efficient therapeutic options. We previously demonstrated that the lack of Cav1 in mice is associated with extensive collagen deposition in cardiac tissues post-injury, and we suggested that failure to re-express Cav1 during the proliferative and maturation phase of post cardiac injury could be associated with heart failure and increased mortality [10]. Our results presented here suggest that Cav1 also plays an important role during the acute phases of inflammation to increase the relative proportion of M2 macrophages. A limitation to the study is the use of the LAD model, which does not mimic the reperfusion therapy frequently used for MI patients. Non-adaptive scar formation leading to heart failure is a pathologic process driven by unbalanced inflammatory responses. Heart failure and mortality after MI remain elevated mostly due to unbalanced inflammatory responses. As such, these results have broad implications for all MI responses.

In conclusion, Cav1 not only affects inflammation post-MI through TGF-β-mediated pathways but also modifies it through other mechanisms that are yet to be studied. Thus, Cav1 might be one of the important modulators in MI-induced pathogenesis and considered to be a potential therapeutic target.

Supplementary Material

Refer to Web version on PubMed Central for supplementary material.

Acknowledgment

This work was financially supported by NIH-NCCAM R00 AT006704 to GVH and R01HL66231 to CHM, National Institutes of Health (NIH)/NIH Heart, Lung and Blood Institute HHSN 268201000036C (N01-HV-00244) for the San Antonio Cardiovascular Proteomics Center and HL075360, from the Biomedical Laboratory Research and Development Service of the Veterans Affairs Office of Research and Development Award 5I01BX000505 to MLL, and Grant-in-aid funds from the American Heart Association (10GRNT4020024) and Janey Briscoe Center of Excellence in Cardiovascular Research (CJLS).

References

1. Hawranek M, Gasior M, Gierlotka M, Wilczek K, Lekston A, Szygula-Jurkiewicz B, et al. Progression of coronary artery atherosclerosis after acute myocardial infarction: an angiographic study. J Invasive Cardiol. 2010; 22(5):209–215. [PubMed: 20440036]
2. Sawabe M, Hamamatsu A, Chida K, Arai T, Harada K, Ozawa T, et al. Elderly patients with minimal common carotid atherosclerosis not infrequently have severe coronary atherosclerosis and myocardial infarction. Circ J. 2008; 72(12):1946–1952. [PubMed: 18931452]
3. Berg K, Jynge P, Bjerve K, Skarra S, Basu S, Wiseth R. Oxidative stress and inflammatory response during and following coronary interventions for acute myocardial infarction. Free Radic Res. 2005; 39(6):629–636. [PubMed: 16036341]
4. Frangogiannis NG, Smith CW, Entman ML. The inflammatory response in myocardial infarction. Cardiovasc Res. 2002; 53(1):31–47. [PubMed: 11744011]
5. Lambert JM, Lopez EF, Lindsey ML. Macrophage roles following myocardial infarction. Int J Cardiol. 2008; 130(2):147–158. [PubMed: 18656272]

6. Hu Y, Zhang H, Lu Y, Bai H, Xu Y, Zhu X, et al. Class A scavenger receptor attenuates myocardial infarction-induced cardiomyocyte necrosis through suppressing M1 macrophage subset polarization. Basic Res Cardiol. 2011; 106(6):1311–1328. [PubMed: 21769674]
7. Tao ZY, Cavasin MA, Yang F, Liu YH, Yang XP. Temporal changes in matrix metalloproteinase expression and inflammatory response associated with cardiac rupture after myocardial infarction in mice. Life Sci. 2004; 74(12):1561–1572. [PubMed: 14729404]
8. Bujak M, Frangogiannis NG. The role of TGF-beta signaling in myocardial infarction and cardiac remodeling. Cardiovasc Res. 2007; 74(2):184–195. [PubMed: 17109837]
9. Thomas CM, Smart EJ. Caveolae structure and function. J Cell Mol Med. 2008; 12(3):796–809. [PubMed: 18315571]
10. Miyasato SK, Loeffler J, Shohet R, Zhang J, Lindsey M, Le Saux CJ. Caveolin-1modulates TGF-beta1 signaling in cardiac remodeling. Matrix Biol. 2011; 30(5–6):318–329. [PubMed: 21641995]
11. Di Guglielmo GM, Le Roy C, Goodfellow AF, Wrana JL. Distinct endocytic pathways regulate TGF-beta receptor signalling and turnover. Nat Cell Biol. 2003; 5(5):410–421. [PubMed: 12717440]
12. Ito T, Williams JD, Fraser DJ, Phillips AO. Hyaluronan regulates transforming growth factor-beta1 receptor compartmentalization. J Biol Chem. 2004; 279(24):25326–25332. [PubMed: 15084590]
13. Fu Y, Moore XL, Lee MK, Fernandez-Rojo MA, Parat MO, Parton RG, et al. Caveolin-1 plays a critical role in the differentiation of monocytes into macrophages. Arterioscler Thromb Vasc Biol. 2012; 32(9):e117–e125. [PubMed: 22772753]
14. Lindsey ML, Escobar GP, Dobrucki LW, Goshorn DK, Bouges S, Mingoia JT, et al. Matrix metalloproteinase-9 gene deletion facilitates angiogenesis after myocardial infarction. Am J Physiol Heart Circ Physiol. 2006; 290(1):H232–H239. [PubMed: 16126817]
15. Gould KE, Taffet GE, Michael LH, Christie RM, Konkol DL, Pocius JS, et al. Heart failure and greater infarct expansion in middle-aged mice: a relevant model for postinfarction failure. Am J Physiol Heart Circ Physiol. 2002; 282(2):H615–H621. [PubMed: 11788410]
16. Kern CB, Norris RA, Thompson RP, Argraves WS, Fairey SE, Reyes L, et al. Versican proteolysis mediates myocardial regression during outflow tract development. Dev Dyn. 2007; 236(3):671–683. [PubMed: 17226818]
17. Norris RA, Damon B, Mironov V, Kasyanov V, Ramamurthi A, Moreno-Rodriguez R, et al. Periostin regulates collagen fibrillogenesis and the biomechanical properties of connective tissues. J Cell Biochem. 2007; 101(3):695–711. [PubMed: 17226767]
18. Schneider CA, Rasband WS, Eliceiri KW. NIH Image to ImageJ: 25 years of image analysis. Nat Methods. 2012; 9(7):671–675. [PubMed: 22930834]
19. Wang H, Melton DW, Porter L, Sarwar ZU, McManus LM, Shireman PK. Altered macrophage phenotype transition impairs skeletal muscle regeneration. Am J Pathol. 2014; 184(4):1167–1184. [PubMed: 24525152]
20. Wang XM, Kim HP, Song R, Choi AM. Caveolin-1 confers antiinflammatory effects in murine macrophages via the MKK3/p38 MAPK pathway. Am J Respir Cell Mol Biol. 2006; 34(4):434–442. [PubMed: 16357362]
21. Jasmin JF, Rengo G, Lymperopoulos A, Gupta R, Eaton GJ, Quann K, et al. Caveolin-1 deficiency exacerbates cardiac dysfunction and reduces survival in mice with myocardial infarction. Am J Physiol Heart Circ Physiol. 2011; 300(4):H1274–H1281. [PubMed: 21297026]
22. Reardon MJ, Carr CL, Diamond A, Letsou GV, Safi HJ, Espada R, et al. Ischemic left ventricular free wall rupture: prediction, diagnosis, and treatment. Ann Thorac Surg. 1997; 64(5):1509–1513. [PubMed: 9386744]
23. Takada A, Saito K, Nagai T, Hamamatsu A, Murai T. When does an infarcted heart rupture? A pathological study of 148 out-of-hospital sudden death cases. Int J Cardiol. 2008; 129(3):447–448. [PubMed: 17692945]
24. Becker RC, Hochman JS, Cannon CP, Spencer FA, Ball SP, Rizzo MJ, et al. Fatal cardiac rupture among patients treated with thrombolytic agents and adjunctive thrombin antagonists: observations from the thrombolysis and thrombin inhibition in myocardial infarction 9 study. J Am Coll Cardiol. 1999; 33(2):479–487. [PubMed: 9973029]

25. Gao XM, Ming Z, Su Y, Fang L, Kiriazis H, Xu Q, et al. Infarct size and post-infarct inflammation determine the risk of cardiac rupture in mice. Int J Cardiol. 2010; 143(1):20–28. [PubMed: 19195725]

26. Niu J, Kolattukudy PE. Role of MCP-1 in cardiovascular disease: molecular mechanisms and clinical implications. Clin Sci (Lond). 2009; 117(3):95–109. [PubMed: 19566488]

27. Ono K, Matsumori A, Furukawa Y, Igata H, Shioi T, Matsushima K, et al. Prevention of myocardial reperfusion injury in rats by an antibody against monocyte chemotactic and activating factor/monocyte chemoattractant protein-1. Lab Invest. 1999; 79(2):195–203. [PubMed: 10068207]

28. Anzai T. Post-infarction inflammation and left ventricular remodeling- a double-edged sword. Circ J. 2013; 77(3):580–587. [PubMed: 23358460]

29. Ikeuchi M, Tsutsui H, Shiomi T, Matsusaka H, Matsushima S, Wen J, et al. Inhibition of TGF-beta signaling exacerbates early cardiac dysfunction but prevents late remodeling after infarction. Cardiovasc Res. 2004; 64(3):526–535. [PubMed: 15537506]

30. Okada H, Takemura G, Kosai K, Li Y, Takahashi T, Esaki M, et al. Postinfarction gene therapy against transforming growth factor-beta signal modulates infarct tissue dynamics and attenuates left ventricular remodeling and heart failure. Circulation. 2005; 111(19):2430–2437. [PubMed: 15867170]

31. Akasaka Y, Morimoto N, Ishikawa Y, Fujita K, Ito K, Kimura-Matsumoto M, et al. Myocardial apoptosis associated with the expression of proinflammatory cytokines during the course of myocardial infarction. Mod Pathol. 2006; 19(4):588–598. [PubMed: 16554734]

32. Frangogiannis NG. Targeting the inflammatory response in healing myocardial infarcts. Curr Med Chem. 2006; 13(16):1877–1893. [PubMed: 16842199]

33. Kevin LG, Novalija E, Stowe DF. Reactive oxygen species as mediators of cardiac injury and protection: the relevance to anesthesia practice. Anesth Analg. 2005; 101(5):1275–1287. [PubMed: 16243980]

34. Dayan V, Yannarelli G, Billia F, Filomeno P, Wang XH, Davies JE, et al. Mesenchymal stromal cells mediate a switch to alternatively activated monocytes/macrophages after acute myocardial infarction. Basic Res Cardiol. 2011; 106(6):1299–1310. [PubMed: 21901289]

35. Anzai A, Anzai T, Nagai S, Maekawa Y, Naito K, Kaneko H, et al. Regulatory role of dendritic cells in postinfarction healing and left ventricular remodeling. Circulation. 2012; 125(10):1234–1245. [PubMed: 22308302]

36. El Kasmi KC, Qualls JE, Pesce JT, Smith AM, Thompson RW, Henao-Tamayo M, et al. Toll-like receptor-induced arginase 1 in macrophages thwarts effective immunity against intracellular pathogens. Nat Immunol. 2008; 9(12):1399–1406. [PubMed: 18978793]

37. Pesce JT, Ramalingam TR, Mentink-Kane MM, Wilson MS, El Kasmi KC, Smith AM, et al. Arginase-1-expressing macrophages suppress Th2 cytokine-driven inflammation and fibrosis. PLoS Pathog. 2009; 5(4):e1000371. [PubMed: 19360123]

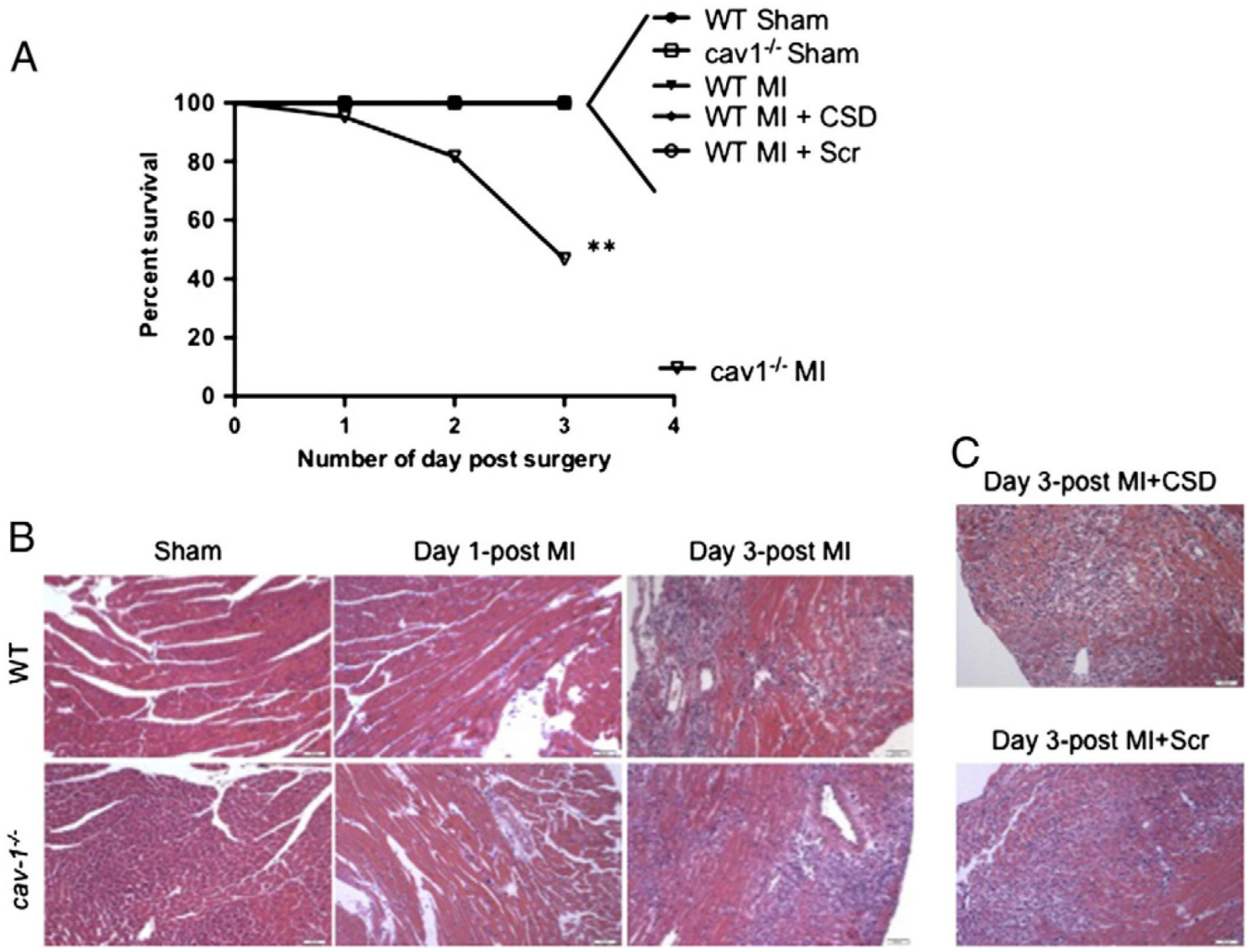

Fig. 1.

Survival and histology post myocardial injury in Wild Type and *Cav1*$^{-/-}$ mice. A) Survival curve of animals post myocardial injury with treatment of CSD or a scrambled peptide. Statistical significance was calculated using a Log-rank (Mantel Cox) test. p-value = 0.0086. B) Representative H&E stained sections of injured cardiac tissues obtained on day 1 and day 3 post-MI from WT and *Cav1*$^{-/-}$mice. C) Representative H&E stained sections of injured cardiac tissues obtained on day 3 post-MI with treatment of CSD or the scrambled control peptide.

A

Cell Types	WT-Sham	WT-MI	WT-MI+Scr	WT-MI+CSD	Cav-1$^{-/-}$-Sham	Cav-1$^{-/-}$-MI
Total Mϕ Mean±SE	31.33±4.37	870.8±400.3 **, #	1580±152.3	2759±400.3 *	24.33±6.89	1299±71.99 **, #
Arginase 1 positive–Mϕ Mean±SE	2.667±1.76	152.11±13.35 ***, #	269.7±21.4	249±20.88 *	00±0.00	270±8.5 ***,#

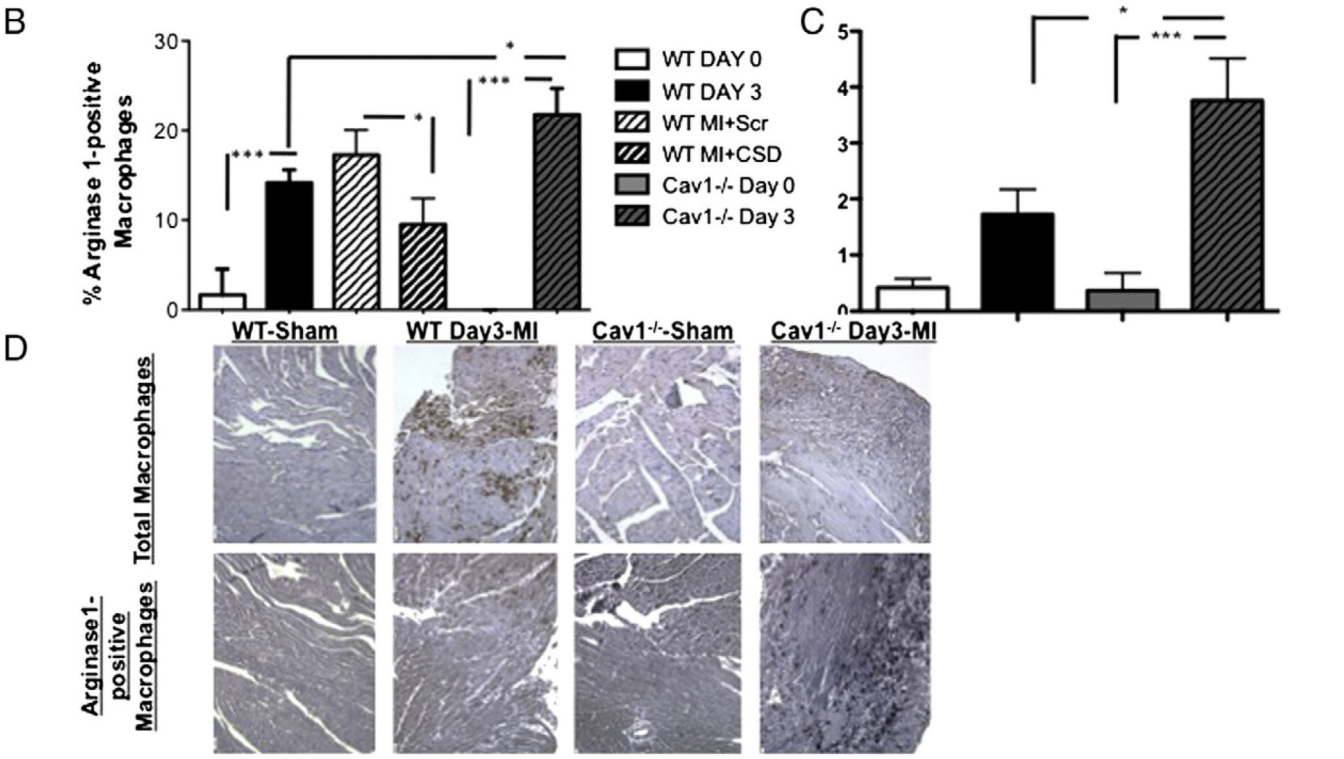

Fig. 2.

Increased M2 macrophage in infarcted area in *Cav1*$^{-/-}$ mice after myocardial injury. A) Left ventricular sections of wild type (WT) and Cav1$^{-/-}$ mice treated with the cav1 scaffolding domain (CSD) or scrambled (Scr) peptide were collected 3 days after myocardial infarction (MI) and probed with anti-mac2 antibody; and M2 macrophage (MΦ) phenotypes probed with anti-arginase-1 antibody. Cell counts of labeled macrophages were obtained and reported as mean± standard error (SE). B) Percentage of arginase-1-positive macrophages in the infarcted area of the hearts of WT and *Cav1*$^{-/-}$ mice 3 days post-MI. C) Relative levels of *Arg-1* mRNA expressions in infarcted heart tissues of WT and *Cav1*$^{-/-}$ mice 3 days post-MI. Fold changes are relative to the 18S ribosomal RNA as internal control. D) Upper panel: Representative photomicrographs of infarcted heart tissue stained with Mac-2 staining to detect macrophages in WT and *Cav1*$^{-/-}$ mice 3 days post-MI. Lower panel: Representative photomicrographs of infarcted heart tissue sections of M2 macrophages detected using Arginase-1 marker in infarcted myocardium of WT and *Cav1*$^{-/-}$mice 3 days post-MI. Statistical significance was obtained using a 2-way ANOVA analysis followed by a Bonferroni post-test: * denotes p-value <0.05; *** p-value <0.001; n = 3 animals per group,

in triplicates [3 sections of 3 μm thickness were fixed on each slide from each mouse tissue sample and each mouse value represented average counts from 3 FOVs].

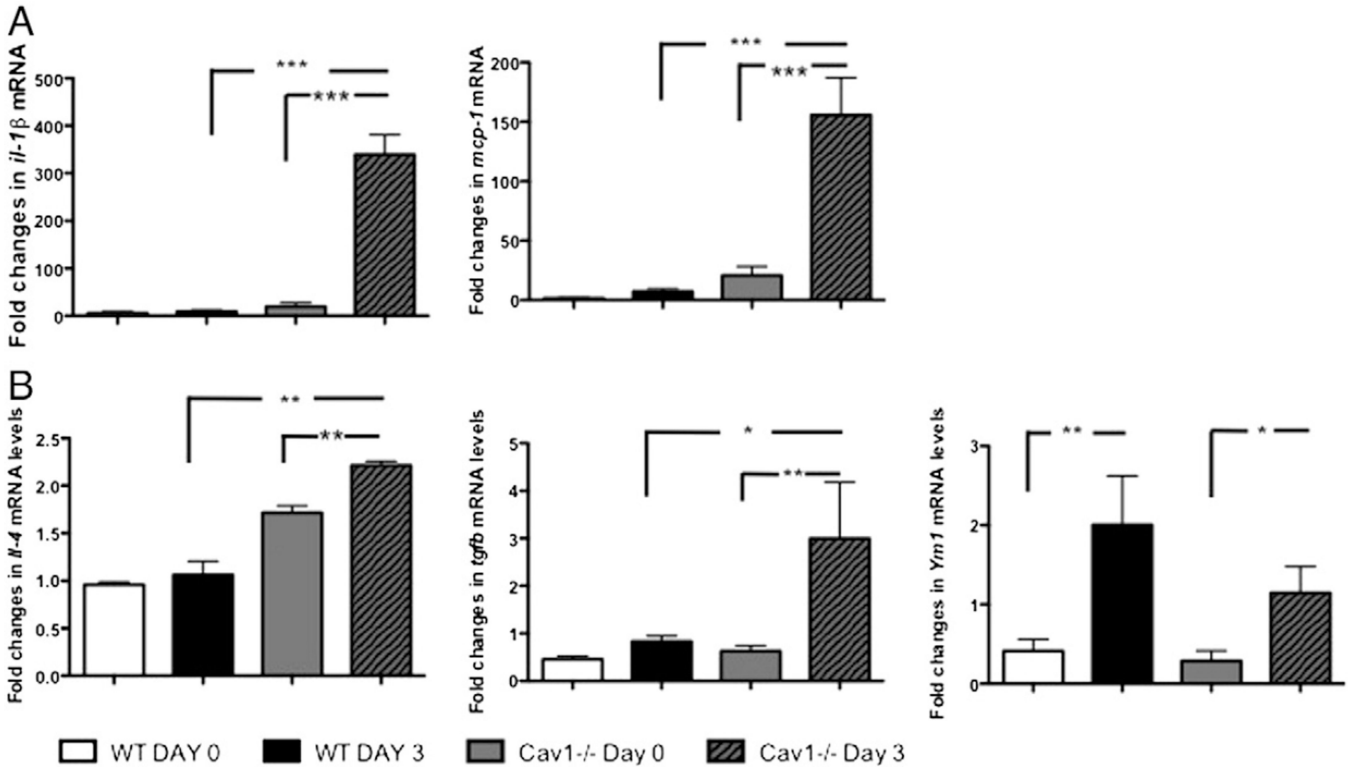

Fig. 3.

Cytokine and chemokine expression. A) Relative levels ofM1macrophage phenotype markers *tnf*α, *il-1*β and *mcp-1* mRNA expressions in infarcted heart tissues of WT and *Cav1*$^{-/-}$ mice 3 days post-MI. B) Relative levels of mRNA of proteins encoding proteins that promote M2 macrophage phenotype (*IL-4* and *TGF*-β) and markers (*TGF*-β and*ym-1*) mRNA expressions in infarcted heart tissues of WT and *Cav1*$^{-/-}$ mice 3 days post-MI. Values are represented relative to 18S ribosomal RNA as internal control. Statistical significance was obtained using a 2-way ANOVA analysis followed by a Bonferroni post-test: * denotes p-value <0.05; *** p-value <0.001; n = 3–5 animals per group, in triplicates. In addition # denotes p-value <0.05 between the 2 strains within the same intervention group.

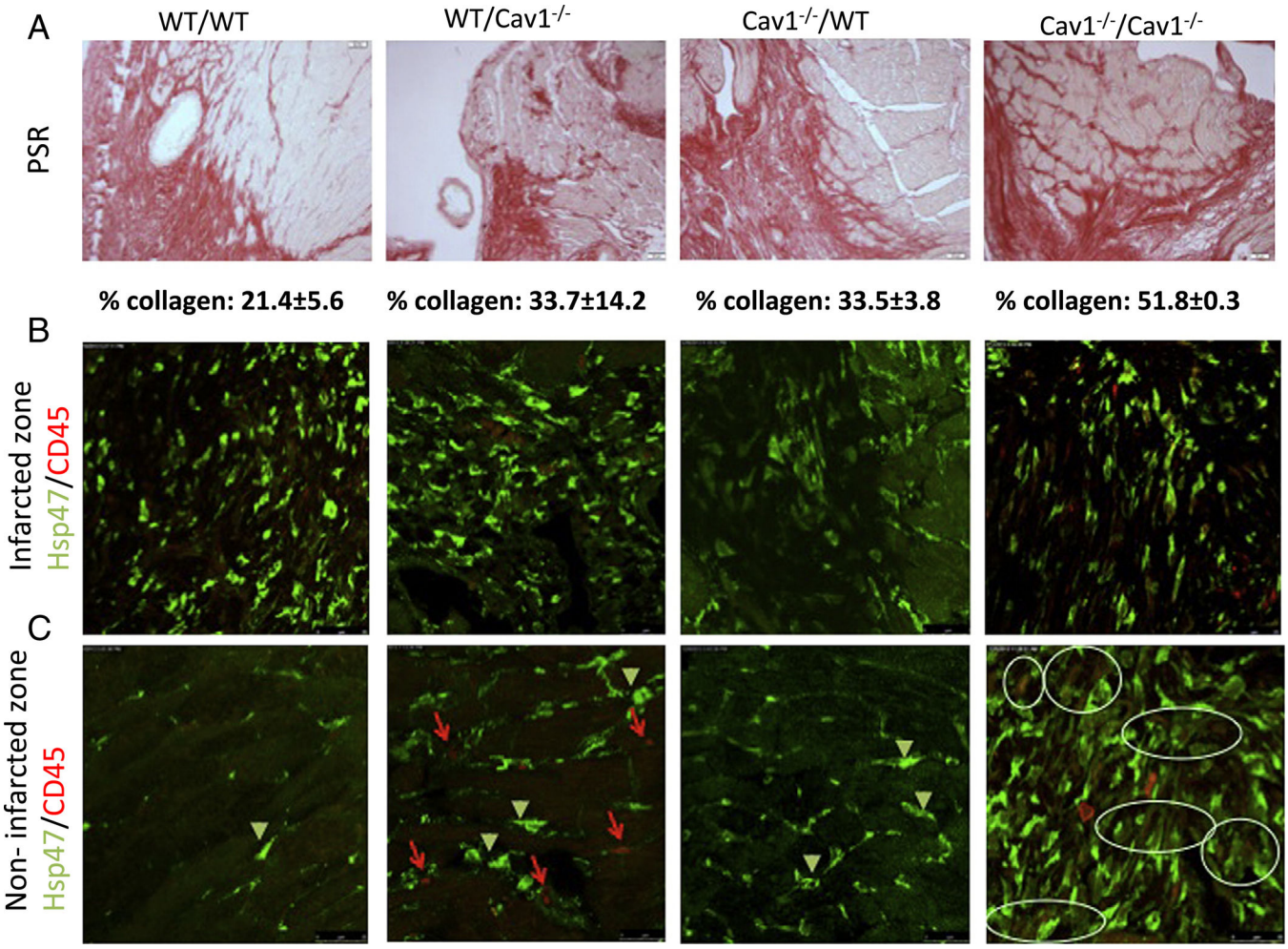

Fig. 4.

Interstitial fibrosis is dampened in Cav1$^{-/-}$ mice by adoptive transfer 3 days after MI of WT macrophages. A) Collagen deposition was detected by picrosirius red staining in the injured zone and myocardium interstitium and quantified (% of collagen) using Image J software 14 days after MI. Representative photomicrographs of cells located at the infarct zone boundary (B) and outside of the infarct zone (C) of heart 14 post-MI showing the detection of fibrocytes (positive for CD45 and Hsp47), indicative of adverse remodeling. Images were obtained with a Leica SP5 confocal microscope. Mag. 1000×. n = 3 per group.

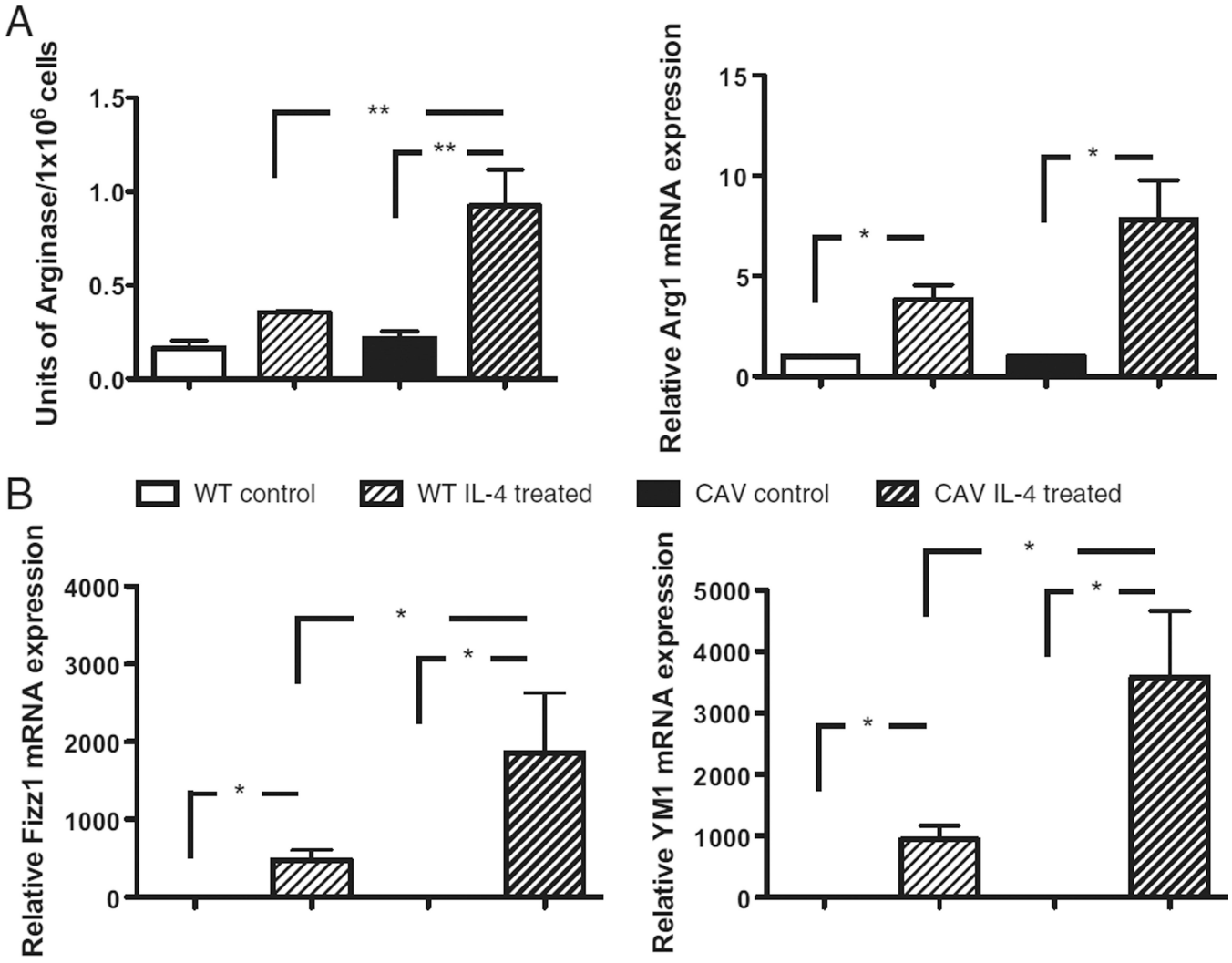

Fig. 5.

In vitro macrophage activation assays. A) Arginase enzymatic assay: Units of native arginase per 1 × 10^6 cells of WT and *Cav1*$^{-/-}$ peritoneal macrophages. Cells were stimulated with 10 ng/ml of IL-4 for 24 h or left untreated. One unit equals the amount of enzyme required to hydrolyze 1 μM arginine per minute. Statistical significance: * denotes p-value <0.05; ** p-value <0.01; n=8 per group. B) Relative levels of M2 macrophage phenotype markers *arg-1*, *fizz-1*, and *ym-1* mRNA expressions in treated peritoneal macrophages from WT and *Cav1*$^{-/-}$ mice as mentioned in (A). Values are represented relative to 18S ribosomal RNA as internal control.

A

TGF-β DEPENDENT GENES	Cav-1 DEPENDENT GENES	TGF-β AND Cav-1 DEPENDENT GENES
Ccl12	CxCl10	IL-11
Ccl20	Ccl11	IL-3
Ccr4	Ccl1	Ccr8
Ccr6	CxCl9	C3
Crp	Ltb	IL-10
CxCl15	Ccl20	IL-4
IL-1r2	Pf4	Ccr9
Itgb2	CxCl5	IL-1α
Spp1	Xcr1	IL-1β
IL-1r1	IL-1f87	CxCl13
		IL-17β
		Ccl24
		TNF-α
		IL-8rβ
		IL-18
		CD40lg
		Lta
		IL-1r2
		IFN-γ
		Bcl6Ccl22
		Ccl1
		CxCr5

B

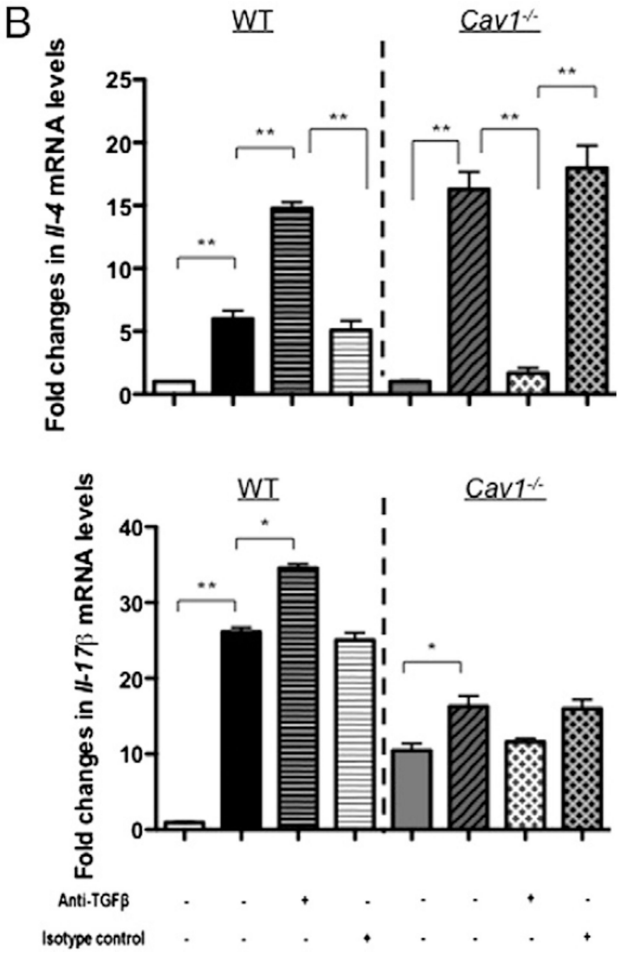

Fig. 6.

TGF-β and Cav-1 dependent and independent regulation of cytokine/chemokine expression 3 days after myocardial injury. A) Representation of transcripts screened by semiquantitative real time PCR array. Transcripts were classified into 3 main categories as TGF-β– and Cav1-dependent only and as dual dependency on genes for their combined functions. B) Relative mRNA levels for *IL-4* and *IL-17b* are shown to be significantly increased in the infracted region of anti-TGF-β antibody treated WT mouse hearts compared to untreated injured hearts. Values presented are relative to the 18S ribosomal RNA as internal control. Statistical significance: * denotes p-value <0.05; ** p-value <0.01; n=3 animals per group, in triplicates.

Cell Types (per FOV)	WT-MI+anti-TGFβ	WT-MI +Isotype control
Total Mφ Mean±SE	927±24.01	570.7±106.2
M2 Mφ Mean±SE	256.2±7.54	393.3±58.72

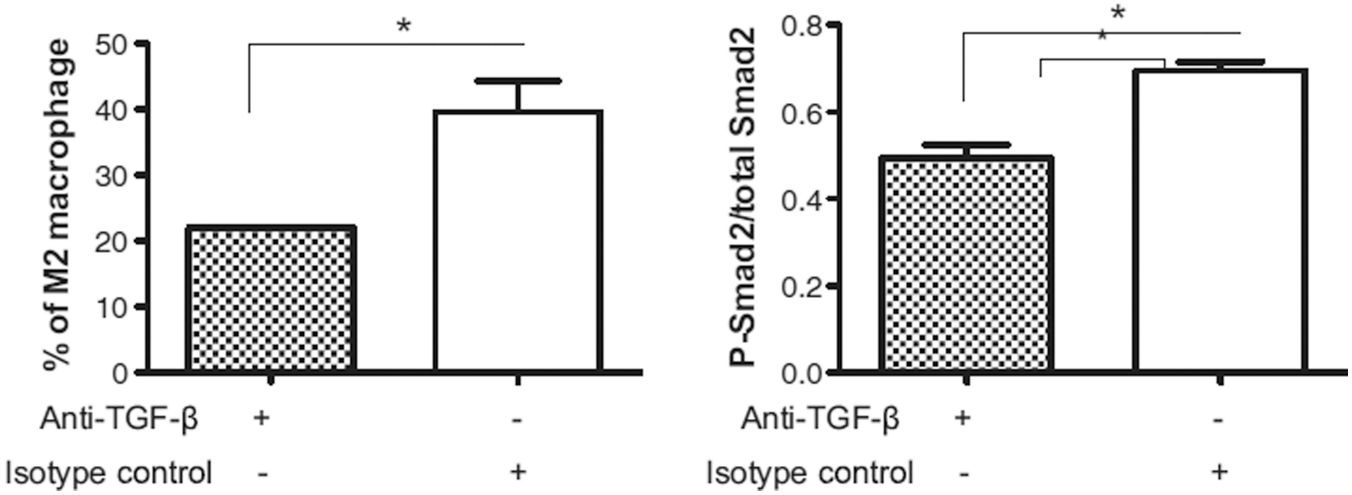

Fig. 7.

Inhibition of TGF-β signaling pathway reduced M2 macrophage counts. A) Macrophage and M2 macrophage detected by Mac-2 and arginase-1 antibody staining were counted in infarcted region in triplicates [3 sections of 3 μm thickness were fixed on each slide from each mouse tissue sample and each mouse value represented average counts from 3 FOVs]. B) Percentage of arginase-1-positive macrophages in the infarcted area of the heart tissues of WT with anti-TGF-β antibody or isotype control for 3 days after myocardial injury. C) Immunoblot analyses of P-Smad2 and Smad2 levels in homogenates of infarcted heart tissues isolated from WT mice treated with anti-TGF-β antibody or isotype control for 3 days after myocardial injury. The histograms represent densitometric quantifications of the relative levels of P-Smad2 to Smad2. Statistical significance: * denotes p-value <0.05; n=3 animals per group.

Table 1

Caveolin-1 deficiency does not affect left ventricle (LV) dysfunction post–myocardial infarction.

		FS (%)	LV infarct wall thinning (d; mm)	EDV (μl)	ESV (μl)	EF (%)
WT	Baseline	34 ± 2	0.7 ± 0.01	52 ± 2	21 ± 2	64 ± 2
	1 day after MI	11 ± 1*	0.5 ± 0.04	83 ± 7	65 ± 7	22 ± 2
	3 days after MI	9 ± 1*	0.5 ± 0.06	91 ± 1	75 ± 4	18 ± 3
Cav1$^{-/-}$	Baseline	29 ± 1	0.7 ± 0.03	42 ± 2	15 ± 2	65 ± 3
	1 day after MI	6 ± 1*	0.4 ± 0.02	71 ± 13	63 ± 11	11 ± 3
	3 days after MI	7 ± 2*	0.4 ± 0.01	82 ± 12	66 ± 14	22 ± 5

* $p < 0.05$ vs. respective baseline.

Abbreviations: WT: wild type mouse; Cav1$^{-/-}$: caveolin-1 deficient mouse; MI: myocardial infarction; FS: Fractional Shortening; d: diastole; EDV: End-Diastolic Volume; ESV: End-Systolic Volume; EF: Ejection fraction.